Wavelength dependence of the photoelectron angular distributions of the rare gases*

J. L. Dehmer, W. A. Chupka,† J. Berkowitz, and W. T. Jivery
Argonne National Laboratory, Argonne, Illinois 60439
(Received 17 July 1975)

Photoelectron angular distributions for the valence p shells of the rare gases have been measured up to a photon energy of 40.8 eV (48.4 eV for Ne) using resonance radiation from a hollow-cathode discharge lamp. This work extends the range of existing absolute measurements on Ne, Kr, and Xe. Comparison with Hartree-Fock and RPAE (random-phase approximation with exchange) calculations indicates excellent agreement for Ne. However, the present results, particularly for Xe, add to earlier evidence that data for Ar, Kr, and Xe show systematic deviations from theory, especially at the higher photoelectron kinetic energies. For Kr and Xe, we report asymmetry parameters separately for processes leading to the $^2P_{3/2,1/2}$ spin-orbit states of the residual ion. The Xe results indicate that $\beta_{3/2}-\beta_{1/2}$ is positive for $\lambda \geq 461$ Å, but changes sign in the range $\lambda \sim 350$–400 Å. At 304 Å, $\beta_{3/2}-\beta_{1/2}=-0.30$, which agrees with a recent calculation based on the Dirac-Slater model.

I. INTRODUCTION

Within the dipole approximation, the angular distribution of photoelectrons ejected from isolated randomly oriented atoms by unpolarized radiation has the simple form[1]

$$\frac{d\sigma}{d\Omega}=\frac{\sigma_{\text{tot}}}{4\pi}[1-\tfrac{1}{2}\beta P_2(\cos\theta)], \tag{1}$$

where σ_{tot} is the integrated cross section, β is the asymmetry parameter, and θ is the ejection angle relative to the incident light beam. Consequently, the anisotropy of the differential photoionization cross section is completely characterized by the parameter β, which contains both geometric (symmetry) and dynamic information on the photoionization process. Theoretical expressions have been formulated for the evaluation of β in a variety of circumstances.[2-5] Each of these formulations exhibits an important characteristic of β, namely, its explicit dependence on the difference in phase between alternative ionization channels, as well as on the respective dipole amplitudes. Therefore, β and the integrated cross section play complementary roles in the interplay between experiment and theory. Clearly, the role of β in this interplay hinges on reliable, *wavelength-dependent* measurements of the asymmetry parameter, which have only begun to emerge in the last couple of years.

Although measurements of angular distributions of photoelectrons from the valence shells of rare gases have been going on for a decade,[6-18] reasonable agreement among different laboratories is confined to more recent measurements.[9-18] Several of these studies[12-18] extend the wavelength dependence of β beyond the traditional Ne I and He I resonance wavelengths. (This is in marked contrast to the study of molecular systems, which is almost completely confined to He I radiation.) The measurements in this latter category, which bear directly on the present work, include (a) absolute measurements[16] on Ne using soft x-ray sources, (b) absolute measurements on Ar (Refs. 17, 18) and Kr (Ref. 17) using synchrotron radiation, and (c) relative measurements[12,13,15] on Ne, Kr, and Xe using synchrotron radiation. Also notable in this context are the relative measurements[19,20] on Ne, Ar, and Kr using "pseudophoton" radiation.

The present work contributes to this body of data in two ways. First, we extend the useful wavelength range of resonance radiation work to 304 Å (256 Å for Ne, which has no Cooper zero near this wavelength) with applications to He, Ne, Ar, Kr, and Xe. This represents the only absolute vacuum-ultraviolet measurements for Ne and Xe for $256<\lambda<584$ Å. Second, for Kr and Xe, we report β values separately for processes leading to the $^2P_{3/2,1/2}$ spin-orbit states of the ion in order to elucidate the effect of spin-orbit interaction on these photoelectron angular distributions at wavelengths shorter than 584 Å.

II. EXPERIMENTAL DETAILS

A schematic diagram of the apparatus is shown in Fig. 1. In the present arrangement, the hemispherical analyzer, shown in the $\theta=90°$ position, can be rotated clockwise in the plane of the figure to $\theta=270°$. The angle is stepped with a Slo-Syn type HS50 stepping motor driven by an ORTEC Model 6713 Axis Controller. (It is also possible to rotate the analyzer out of the horizontal plane; however, this capability is not required in this work.) The light is channeled into the interaction

region through a 2-mm Pyrex capillary tube, supported by a holder which is coupled to the rotating analyzer by a sapphire-ball bearing mounted on the entrance lens. The target gas is introduced into the interaction region through a molybdenum jet, which terminates in a single 0.020-in. diameter $\times$0.125-in. channel positioned ~0.050 in. below the center of the light beam. This crossed-beam configuration produces a source of photoelectrons which is symmetric about the axis of rotation, thus eliminating the need for source-geometry corrections.

The hemispherical spectrometer has a mean radius of 2.25 in. and is fabricated from oxygen-free high-conductivity copper. The entrance optics consist of an entrance aperture of 0.040 in. (0.060 in. for He II measurements), a three-aperture lens operated as a "zoom" lens,[21] two pairs of deflectors, and a Herzog lens.[22] The entrance optics are fabricated from molybdenum. With the 0.040-in. entrance aperture, the resolving power, $\Delta E/E$, is ~1.5%. The exit optics consist of a Herzog lens and a simple two-cylinder lens. During these experiments, a constant kinetic energy of 10 eV was used in the dispersive element, the zoom lens being adjusted to focus the photoelectrons studied on the entrance plane of the hemispheres with this kinetic energy. All surfaces exposed to the electron beam are coated with colloidal graphite to achieve a uniform surface potential and reduce scattered-electron background.

A hollow-cathode discharge lamp is used to produce He I, He II, Ne I, and Ne II resonance lines. The present lamp is similar to one described elsewhere,[23] except that the cathode has been extended outside the back plate and water cooled. The lamp is operated in a dc mode with a typical current of 0.75–1.00 A, and at pressures of ~1 Torr (for He I and Ne I), ~0.15 Torr (for Ne II), and ~0.3 Torr (for He II). Photon fluxes were of the order of 10^{10} sec^{-1} mm^{-2}.

The general operating conditions are as follows. The earth's magnetic field is attenuated by three layers of μ-metal, resulting in a residual field of less than 0.012 G. The background sample-gas pressure in the chamber is chosen to ensure that less than 0.5% of the photoelectrons were scattered from their initial trajectories before angle selection. Typical background pressures are $1-5\times10^{-5}$ Torr, which corresponds to approximately $1-5\times10^{-3}$ Torr in the collision region. During the course of an experiment, a photoelectron peak of interest is recorded with 1% counting statistics at 15–20 angles in the range $90\leq\theta\leq225°$. (The angular distribution was observed to be distorted in the range $225\leq\theta\leq270°$ owing to an inadequately shielded port.) Frequent measurements are made at $\theta=90°$ to monitor the system's stability and to provide a reference intensity for normalizing the integrated counts at the other angles. The resulting data are fitted with the form in Eq. (1) by a least-squares procedure.

The validity of the experimental procedure was checked by measuring the β for He at 304 Å, which should have a value $\beta=2$, characteristic of photoionization of an s electron in the absence of anisotropic interactions involving the outgoing electron. The results of all the measurements taken during the course of this work are shown in Fig. 2, where

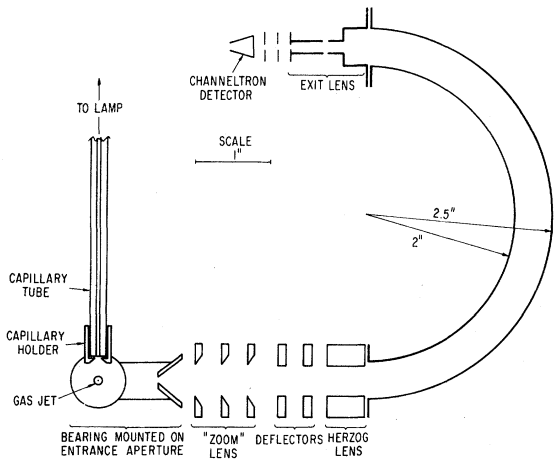

FIG. 1. Schematic diagram of the experimental apparatus.

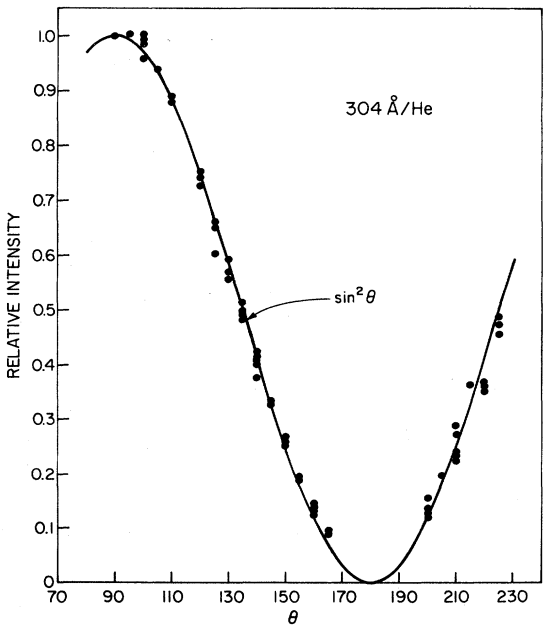

FIG. 2. Photoelectron angular distribution for He at 304 Å.

the solid line denotes the theoretical $\sin^2\theta$ distribution. Analysis of these data results in a value of $\beta = 1.97 \pm 0.04$, indicating the accuracy in β at this kinetic energy to be ~0.05. Moreover, the data in Fig. 2 include measurements made with both the 0.040- and the 0.060-in. apertures and at pressures differing by factors of 2 times and $\frac{1}{2}$ times the normal operating conditions, indicating the absence of effects that are due either to angular resolution or electron scattering under the experimental conditions used here.

III. RESULTS

We divide our discussion of results into two parts. In the first part, we focus on the comparison of our data with other data obtained with resonance radiation. This comparison serves as a convenient check on the accuracy of our results for $\lambda > 584$ Å, where our work overlaps with others. In the second part, we emphasize the wavelength dependence of our results through a comparison with data from synchrotron radiation sources and with theoretical results based on Hartree-Fock (HF) and random-phase approximation with exchange (RPAE) calculations.

Table I lists all the β values we have measured for the rare gases. For comparison, we list the recent results of Niehaus and Ruf[11] and Carlson and Jonas.[10] More extensive comparisons presented in Refs. 10 and 11 indicate large discrepancies with earlier work which, in view of the rather good agreement among recent results, would seem to indicate that the earlier work was subject to significant experimental errors.

Since the difficulty of angular-distribution measurements due, e.g., to residual magnetic and electric fields, varies inversely with photoelectron kinetic energy, we start with the higher energies. For Xe at 584 Å, the present results agree within stated errors with those of Niehaus and Ruf (note that the stated errors represent the standard deviation of the least-squares fit to the data and are therefore a lower limit for the absolute error in the measurements) and are systematically higher by ~0.3 than those of Carlson and Jonas. Considering the rather large photoelectron kinetic energies of 7.78 and 9.10 eV produced in this ionization process, and in view of the superior agreement between the three sets of data for He I on Ar and Kr, we tentatively attribute the low β value observed by Carlson and Jonas to scattering of the photoelectrons by the background gas (10^{-2} Torr in the Carlson and Jonas experiment) before angle selection. This effect, which is particularly strong for Xe and these kinetic energies ($\sigma_{tot} \sim 40\pi a_0^2$), has the effect of lowering the anisotropy of the observed distribution and thus the value of β. This is the worst case among those considered here; however, the systematically lower values of β reported by Carlson and Jonas are probably attributable to the relatively high pressure used in their experiments.

For Ar and Kr at 584 Å, the present results lie between the two earlier sets of data, usually within the sum of the stated errors. For the case of ionization of Xe by Ne I radiation, very good agreement is again observed between the present results and those of Niehaus and Ruf with the Carlson and Jonas value lying ~0.1 lower. For Ne I on Kr, a spread exists between three sets of data which is well outside the stated minimum errors, although the $^2P_{3/2}$-$^2P_{1/2}$ difference for our results agrees well with that measured by Niehaus and Ruf. Note that the photoelectron kinetic energy is ~2 eV for this case, so that the significant spread in β values may arise from the effect of stray fields. For Ar, the discrepancy persists as the photoelectron kinetic energy decreases further.

On the basis of this comparison among the three sets of data, together with our He checks, we conclude that, for kinetic energies *above* ~3 eV, our results are generally accurate to ~0.05–0.10. Moreover, the axially symmetric source geometry achieved in the present experiment avoided the use of the source-geometry correction used by Niehaus and Ruf and by Carlson and Jonas. Hence, our results are free from any error associated with the approximate $\sin\theta$ correction factor applied to the raw data by the other workers.

For lower kinetic energies, the data are scattered over a range of ~0.2–0.4. The absolute measurements[17,18] on Ar and Kr using synchrotron radiation help clarify this discrepancy somewhat, as discussed below. In any case, our new measurements for $\lambda < 584$ Å should be at least as accurate as the $\lambda = 584$ Å results.

In Fig. 3 we compare our Ne data with the relative measurements of Lynch *et al.*[13] using synchrotron radiation, with those of Wuilleumier and Krause[16] using soft x-ray lines, and with HF and RPAE calculations. First we will consider briefly the comparison between the theoretical models. For $2p$ photoionization in Ne, many-electron correlations do not play as important a role as they do in the valence excitation of the heavier noble gases. Moreover, spin-orbit coupling is small so that *LS* coupling is a reasonable approximation. Consequently, good agreement is obtained between the three most commonly used models—Hartree-Slater (HS),[24] HF,[25] and RPAE[26]—each of which employs the Cooper-Zare expression[2] for β in terms of dipole matrix elements and phase shifts. The HF-length (HFL) and HF-velocity (HFV) re-

TABLE I. Comparison of β values for the rare gases obtained with resonance radiation.

Ion	State	λ (Å)	$\hbar\omega$ (eV)	KE (eV)	β values Present	Niehaus and Ruf (Ref. 11)	Carlson and Jonas (Ref. 10)
He^+	$^2S_{1/2}$	462	26.86	2.28	1.96 ± 0.14	•••	•••
He^+	$^2S_{1/2}$	304	40.81	16.23	1.97 ± 0.04	•••	•••
Ne^+	$^2P_{3/2,1/2}$	462	26.86	5.25	0.12 ± 0.05	•••	•••
Ne^+	$^2P_{3/2,1/2}$	304	40.81	19.20	0.81 ± 0.05	•••	•••
Ne^+	$^2P_{3/2,1/2}$	256	48.37	26.76	1.00 ± 0.06	•••	•••
Ar^+	$^2P_{1/2}$	744	16.67	0.73	0.08 ± 0.05	0.25 ± 0.05	0.2 ± 0.2
Ar^+	$^2P_{1/2}$	736	16.85	0.91		0.26 ± 0.03	•••
Ar^+	$^2P_{3/2}$	744	16.67	0.91			
Ar^+	$^2P_{3/2}$	736	16.85	1.09		0.31 ± 0.03	0.4 ± 0.2
Ar^+	$^2P_{1/2}$	584	21.22	5.28	0.89 ± 0.04	0.95 ± 0.02	0.85 ± 0.05
Ar^+	$^2P_{3/2}$	584	21.22	5.46		0.95 ± 0.02	0.85 ± 0.05
Ar^+	$^2P_{3/2,1/2}$	462	26.86	11.01	1.35 ± 0.06	•••	•••
Ar^+	$^2P_{3/2,1/2}$	304	40.81	24.96	1.77 ± 0.04	•••	•••
Kr^+	$^2P_{1/2}$	744	16.67	2.00	0.93 ± 0.05	0.72 ± 0.04	•••
Kr^+	$^2P_{1/2}$	736	16.85	2.18		0.79 ± 0.03	0.58 ± 0.1
Kr^+	$^2P_{3/2}$	744	16.67	2.67	1.05 ± 0.05	0.83 ± 0.04	•••
Kr^+	$^2P_{3/2}$	736	16.85	2.85		0.91 ± 0.03	0.60 ± 0.1
Kr^+	$^2P_{1/2}$	584	21.22	6.55	1.25 ± 0.05	1.37 ± 0.03	1.20 ± 0.05
Kr^+	$^2P_{3/2}$	584	21.22	7.22	1.29 ± 0.05	1.37 ± 0.02	1.20 ± 0.05
Kr^+	$^2P_{1/2}$	462	26.86	12.20	1.50 ± 0.06	•••	•••
Kr^+	$^2P_{3/2}$	462	26.86	12.86	1.60 ± 0.05	•••	•••
Kr^+	$^2P_{1/2}$	304	40.81	26.14	1.93 ± 0.06	•••	•••
Kr^+	$^2P_{3/2}$	304	40.81	26.81	1.90 ± 0.07	•••	•••
Xe^+	$^2P_{1/2}$	744	16.67	3.23	1.23 ± 0.04	1.20 ± 0.08	•••
Xe^+	$^2P_{1/2}$	736	16.85	3.41		1.29 ± 0.04	1.15 ± 0.05
Xe^+	$^2P_{3/2}$	744	16.67	4.55	1.39 ± 0.04	1.37 ± 0.06	•••
Xe^+	$^2P_{3/2}$	736	16.85	4.73		1.45 ± 0.03	1.28 ± 0.05
Xe^+	$^2P_{1/2}$	584	21.22	7.78	1.63 ± 0.05	1.64 ± 0.06	1.35 ± 0.05
Xe^+	$^2P_{3/2}$	584	21.22	9.10	1.77 ± 0.05	1.71 ± 0.02	1.45 ± 0 05
Xe^+	$^2P_{1/2}$	462	26.86	13.42	1.86 ± 0.05	•••	•••
Xe^+	$^2P_{3/2}$	462	26.86	14.74	1.98 ± 0.04	•••	•••
Xe^+	$^2P_{1/2}$	304	40.81	27.37	1.58 ± 0.03	•••	•••
Xe^+	$^2P_{3/2}$	304	40.81	28.69	1.28 ± 0.03	•••	•••

sults are shown together with the RPAE results in Fig. 3. The agreement between the three is very good except for kinetic energies below ~0.2 Ry, where the HF results exhibit minima while the RPAE results decline monotonically toward zero kinetic energy. The HS results, not shown here, agree with the HF curves throughout the range shown. Therefore Ne is a poor system to use for testing the quality of the three models, since the most discriminating test would consist of measurements on photoelectrons within 1 to 2 eV of the ionization threshold, where experimental difficulties are greatest. The single point in this range by Lynch *et al.*[13] is inadequate to distinguish between models; and, at present, no other data exist in this range.

The three sets of experimental results are all in good agreement with theory and each other, indicating that the β for Ne $2p$ photoionization is well characterized over a broad energy range. This system, therefore, represents a good secondary standard for checking angular distribution instruments, since Ne has a rather large photoionization cross section, which remains reasonably flat over a large energy range.[16] The best checks of theory in this case are the absolute measurements presented here and in Ref. 16. The shape of the curve by Lynch *et al.* is also in good agreement with theory; however, these measurements were relative and were normalized to $\beta = 0$ at a kinetic energy of 5 eV to achieve agreement with the HF results. Not shown are the relative measurements of van der Wiel and Brion,[19] who measured the energy loss of forward-scattered high-energy electrons as a "pseudophoton" source. They normalized their results to the HF curve at 20 eV kinetic energy and also achieved good agreement with the HF calculations.

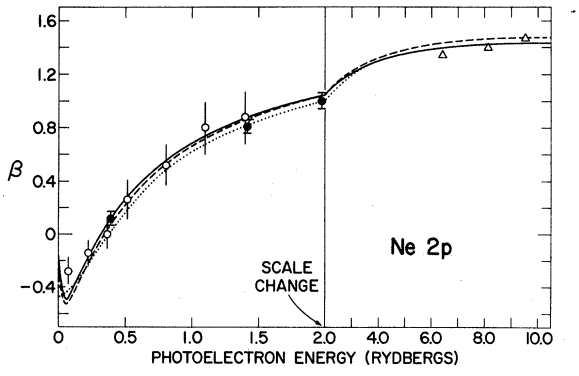

FIG. 3. Energy dependence of β for the $2p$ subshell of Ne: ● (present work); ○ (Lynch *et al.*, Ref. 13); △ (Wuilleumier and Krause, Ref. 16); — HFL, Ref. 25); --- (HFV, Ref. 25); ···· (RPAE, Ref. 26).

The photoelectron angular distribution for the $3p$ subshell of Ar has been studied more extensively than any other case. In addition to the resonance-line work discussed above, there exist five independent measurements of the asymmetry parameter for this process over a broad energy range. These include the relative measurements of Mitchell and Codling[12] using synchrotron radiation, the absolute measurements of Watson and Stewart[17] and of Houlgate *et al.*[18] using synchrotron radiation, and the pseudophoton work of Branton and Brion.[20] We have compared our data with the two recent absolute measurements in Fig. 4, where we have also included curves representing HFL,[25] HFV,[25] and RPAE[26] calculations.

It is apparent in Fig. 4 that Ar is a better test of theoretical models than Ne since, for kinetic energies above ~1.5 Ry, the HF and RPAE curves differ significantly. The HS curve is not shown in Fig. 4 but is known[25] to reach a maximum of β ~1.8 at a kinetic energy of ~1 Ry and then to decline faster than the RPAE curve in Fig. 4. Hence, the RPAE curve lies in between the HS and HF curves, but is much closer to the HF result. That the models agree less well for Ar than for Ne is a consequence of the shape resonance and subsequent Cooper zero in the $3p \rightarrow \epsilon d$ channel of the $3p$ photoionization process. The interaction between the photoelectron and the $3p$ vacancy is very strong in this process and is treated differently in the three models, hence the different results. The data by Houlgate *et al.*[18] show very clearly the superiority of the RPAE results for this case. At the same time, the experimental curve shows a systematic shift toward lower kinetic energy in the region of 2 Ry. Another departure which ap-

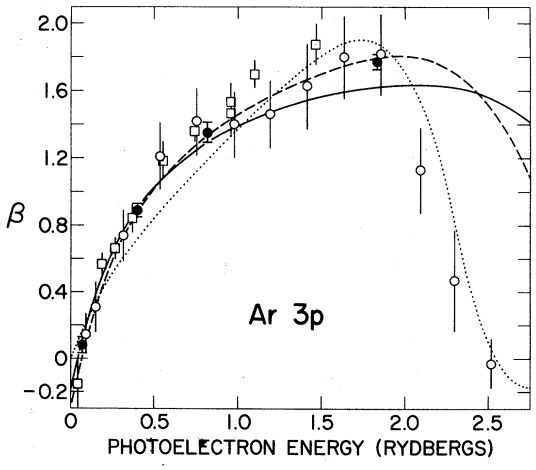

FIG. 4. Energy Dependence of β for the $3p$ subshell of Ar: ● (present work); ○ (Houlgate *et al.*, Ref. 18); □ (Watson and Stewart, Ref. 17); — HFL, Ref. 25); --- (HFV, Ref. 25); · · · · (RPAE, Ref. 26).

pears to be significant occurs at ~0.5–0.75 Ry in Fig. 4. Here, all three sets of data lie above the RPAE result. Our data on Kr and Xe indicate that this tendency for the experimental data to lie above above the RPAE curve at low kinetic energy increases in the heavier rare gases. The tendency to decline faster than the RPAE result is also shown to occur in these heavier rare gases.

Focusing on the experimental results alone, we see all three sets of data are in good agreement. In particular, where our points occur, extremely good agreement exists. Specifically, our Ne I point agrees very well with the nearby points in Fig. 4, whereas the values of $\beta = 0.25$ and 0.2 reported in Refs. 11 and 10, respectively, seem somewhat too high. The maximum scatter in Fig. 4 occurs in the range 1.0–1.6 Ry. Here, the differences of ~0.2 between Houlgate *et al.*[18] and Watson and Stewart[17] are significant, although within their stated error. Moreover, Houlgate *et al.* indicate a plateau between 0.75 and 1.20 Ry, which is not suggested by the data of Watson and Stewart. This incipient structure is absent from the theoretical curves and may be caused by interaction with the $6s^26p^6 \rightarrow 6s6p^6\epsilon p$ channel which opens up in this range. This range could be usefully reexamined to resolve this difference and possibly exhibit the effect of channel interaction near the 6*s* threshold.

The good agreement in Fig. 4 at ~2.0 Ry bears also on the pseudophoton data. Generally, the agreement between the absolute synchrotron data[17,18] and the relative pseudophoton data[20] is good, although significant differences do exist, e.g., in the neighborhood of 22-eV kinetic energy, the pseudophoton data show the beginning of a rapid decrease in β which occurs several volts higher in the measurement of Houlgate *et al.* At 304 Å we obtain a value of $\beta = 1.77$, which indicates that the rapid decline has not yet begun at 25 eV and therefore supports the synchrotron work. For comparison, the pseudophoton data give a value of $\beta \simeq 0.8$ at 25 eV.

In Fig. 5 we compare our results for Kr with the relative data by Lynch *et al.*[15,27] and the absolute data by Watson and Stewart,[17] the latter two measured with synchrotron radiation. Also included are HF[25] and RPAE[26] theoretical results. The relative data by Lynch *et al.* were normalized to $\beta = 1.10$ at 4 eV kinetic energy and generally agree with RPAE results, although significant deviations from the shape of the theoretical curves exist locally. A somewhat different picture emerges from the absolute data which, in the range 0.5–2.0 Ry, agree very well with one another and with the shape of the theoretical curves, but which systematically lie above the theoretical curves. We believe that the data are of sufficient quality to indicate the trend, very marginally observed in Ar, for experimental data to be greater than the HF or RPAE predictions at low kinetic energies. The range of the photon data for Kr is presently insufficient to exhibit the possible deviation from theory at higher energy analogous to that observed for Ar; however, it shows up clearly in the pseudophoton data of Branton and Brion.[20]

A troublesome point in Fig. 5 is the disagreement between our 740 Å points and the data by Watson and Stewart below ~0.4 Ry. The synchrotron data near 0.5 Ry agree very well with our 584 Å data, but then decline more abruptly to approach the theoretical curves which lie close together. At 740 Å, a large spread of $\Delta\beta \sim 0.35$ exists among the four most recent absolute measurements. This spread is difficult to explain, since we know of no autoionization lines in this region and since the total electron scattering cross section of Kr is relatively small for electrons of ~2 eV kinetic energy. It is probable that the sensitivity of 2-eV electrons to residual electric and/or magnetic fields is a main contributor to this spread. Note that the Niehaus and Ruf data would also lie above the theoretical curves although still ~0.15 below our points.

We have also recorded separate values of β corresponding to the $^2P_{3/2,1/2}$ final ionic states of Kr^+. For longer wavelengths, the $\beta_{3/2}$ "curve" seems shifted slightly higher than the $\beta_{1/2}$ "curve," whereas at 304 Å, this order reverses. For Kr, this trend is highly questionable, since the $\beta_{3/2} - \beta_{1/2}$ "shift" is approximately equal to the error bars; however, the same trend is observed to be more

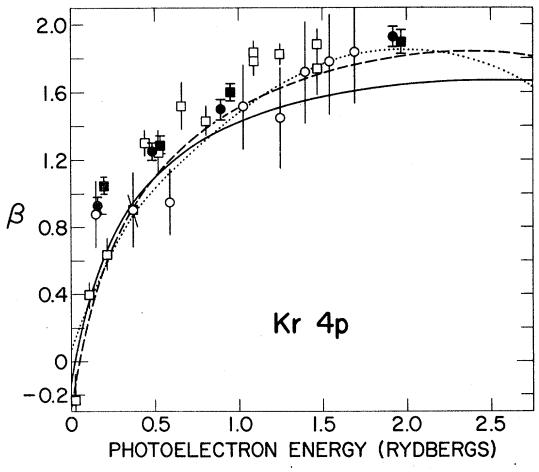

FIG. 5. Energy dependence of β for the 4*p* subshell of Kr: ● ($^2P_{1/2}$, present work); ■ ($^2P_{3/2}$, present work); ○(Lynch *et al.*, Ref. 15); □ (Watson and Stewart, Ref. 17); — (HFL, Ref. 25); --- (HFV, Ref. 25); · · · · (RPAE, Ref. 26).

pronounced in Xe (we shall describe the theoretical results[28] bearing on this crossover in connection with Xe). Verification of this trend must await future, high-precision work emphasizing the effect of spin-orbit coupling on β in heavier atoms.

In Fig. 6 we compare our Xe data with the relative data of Lynch *et al.*[15,27] and the HF and RPAE results. No other absolute measurements have been made for $\lambda < 584$ Å. The comparison between the present work and the theoretical curves prompts two remarks. First, for Xe, the absolute data are higher than the HF and RPAE theories for lower kinetic energies and decrease more rapidly after the maximum at ~1.5 Ry. Hence, although RPAE and HF theory reproduce experiment reasonably well in this wavelength range, room for significant improvement still exists. Second, a significant difference exists between the asymmetry parameters corresponding to the fine-structure levels of the residual ion. Although the main kinetic energy dependence of the spin-orbit effect has been removed in Fig. 6 by plotting β as a function of kinetic energy, the $\beta_{3/2}$ and $\beta_{1/2}$ parameters apparently track on different curves which are separated by ~0.05. In addition, the $\beta_{3/2}$ curve is above the $\beta_{1/2}$ curve below ~1.5 Ry, but then a crossover takes place so that at 304 Å, $\beta_{3/2} < \beta_{1/2}$. It could be argued that owing to the very steep descent of β near 304 Å, the kinetic energy difference would account for this. However, this would require a slope of ~ -3 Ry^{-1}, whereas the HS model, which we feel represents an extreme limit in this case, has a maximum slope of ~ -1 Ry^{-1}. Only a more extensive mapping of the β parameter for the spin-orbit substates in this energy range will establish this conclusively.

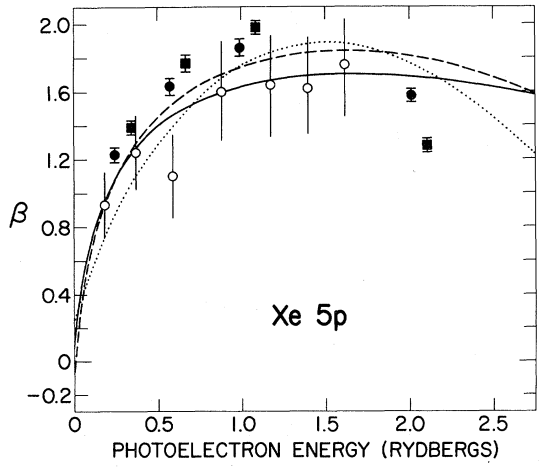

FIG. 6. Energy dependence of β for the 5p subshell of Xe: ●($^2P_{1/2}$, present work); ■ ($^2P_{3/2}$, present work); ○ (Lynch *et al.*, Ref. 15); — (HFL, Ref. 25); --- (HFV, Ref. 25); · · · · (RPAE, Ref. 26).

The only theoretical work pertaining to this effect of spin-orbit coupling in Xe is a Dirac-Slater calculation by Walker and Waber.[28] Their calculation gives $\beta_{3/2} - \beta_{1/2} < 0$ in this energy range; however, the same trend is indicated for lower kinetic energy as well, which disagrees with experiment. Unfortunately, this theoretical work employs a statistical treatment of exchange which is known from nonrelativistic work[25] to yield only qualitative or semiquantitative results. Nevertheless, this approximate calculation, together with our measurements, suffices to indicate that spin-orbit coupling may have a measurable effect on the photoelectron angular distributions for heavier atoms.

IV. CONCLUSIONS

The combination of the present work and the large body of previous work on the photoelectron angular distributions of the rare gases leads to the following conclusions. For photoelectron kinetic energies below ~10 Ry, very good agreement between experiment and theory exists in the case of Ne. For Ar, Kr, and Xe, on the other hand, significant deviations persist between experiment and the most accurate theoretical method presently in use, RPAE. Specifically, the experimental data generally tend to lie above the RPAE curve between threshold and the first maximum in β at ~1.5 Ry. Beyond this maximum, experimental data decrease to the next minimum more rapidly than predicted by theory. The first of these effects is much weaker than the latter, which has been clearly demonstrated for Ar,[18,20] Kr,[20] and, in the present work, for Xe. One schematic way to describe these systematic departures from RPAE is to say they tend slightly toward the HS result, although we attach no significance to this observation. In any case, it is clear from the present body of data that there remains room for sizable refinements in theory. The most significant experimental advancement would be to extend the present body of data to shorter wavelengths to map out the higher-energy structure in β predicted by theory.[25]

We have also brought attention to a facet of this field which requires further development—the effect of spin-orbit coupling. Our measurements on Xe appear to indicate that the β curves corresponding to the two spin-orbit substates of the residual ion are displaced from one another and that they cross near the first maximum in β above threshold. More extensive data are required to document this effect fully. The theory of spin-orbit

effects in this context is also in a relatively primitive stage. Although expressions for β have been developed in the limit of *jj* coupling, the only calculations[28] based on this formulation have employed a statistical exchange approximation, resulting in poor agreement with experiment. This should be rectified by adding spin-orbit coupling to the HF or RPAE schemes.

---

*Work performed under the auspices of the U. S. Energy Research and Development Administration.

†Present address: Dept. of Chemistry, Yale University, New Haven, Conn. 06520.

[1]C. N. Yang, Phys. Rev. 74, 764 (1948).

[2]J. Cooper and R. N. Zare, J. Chem. Phys. 48, 942 (1968); and in *Lectures in Theoretical Physics*, edited by S. Geltman, K. Mahanthappa, and N. Brittin (Gordon and Breach, New York, 1969), Vol. 11c, p. 317.

[3]U. Fano and Dan Dill, Phys. Rev. A 6, 185 (1972).

[4]T. E. H. Walker and J. T. Waber, J. Phys. B 6, 1165 (1973).

[5]D. Dill, A. F. Starace, and S. T. Manson, Phys. Rev. A 11, 1596 (1975).

[6]J. Berkowitz and H. Ehrhardt, Phys. Lett. 21, 531 (1966); and J. Berkowtiz, H. Ehrhardt, and T. Tekaat, Z. Phys. 200, 69 (1967).

[7]J. W. McGowan, D. A. Vroom and A. R. Comeoux, J. Chem, Phys. 51, 5626 (1969).

[8]J. A. R. Samson, Philos. Trans. R. Soc. Lond. A 268, 141 (1970).

[9]R. Morgenstern, A. Niehaus, and M. W. Ruf, Chem. Phys. Lett. 4, 635 (1970).

[10]T. A. Carlson and A. E. Jonas, J. Chem. Phys. 55, 4913 (1971).

[11]A. Niehaus and M. W. Ruf. Z. Phys. 252, 84 (1972).

[12]P. Mitchell and K. Codling, Phys. Lett. 38A, 31 (1972).

[13]M. J. Lynch, A. B. Gardner and K. Codling, Phys. Lett. 40A, 349 (1972).

[14]J. A. R. Samson and J. L. Gardner, Phys. Rev. Lett. 31, 1327 (1973).

[15]M. J. Lynch, K. Codling, and A. B. Gardner, Phys. Lett. 43A, 213 (1973).

[16]F. Wuilleumier and M. O. Krause, Phys. Rev. A 10, 242 (1974).

[17]W. S. Watson and D. T. Stewart, J. Phys. B 7, L466 (1974).

[18]R. G. Houlgate, J. B. West, K. Codling, and G. V. Marr, J. Phys. B 7, L470 (1974).

[19]M. J. van der Wiel and C. E. Brion, J. Electron Spectrosc. 1, 439 (1973).

[20]G. R. Branton and C. E. Brion, J. Electron Spectrosc. 3, 123 (1974).

[21]F. H. Read, J. Sci. Instrum. 3, 127 (1970).

[22]R. Herzog, Z. Phys. 97, 596 (1935).

[23]J. L. Dehmer and J. Berkowitz, Phys. Rev. A 10, 484 (1974).

[24]F. Herman and S. Skillman, *Atomic Structure Calculations* (Prentice-Hall, Englewood Cliffs, N. J., 1963).

[25]D. J. Kennedy and S. T. Manson, Phys. Rev. A 5, 227 (1972).

[26]M. Ya. Amusia, N. A. Cherepkov, and L. V. Chernysheva, Phys. Lett. 40A, 15 (1972).

[27]The Kr points in Fig. 5 differ from those in Ref. 15. The data used there has been corrected to achieve a consistent electron analyzer efficiency, first-to-second order ratio for the grazing incidence spectrometer, and background-gas scattering factor. The corrected data appear in a thesis by A. B. Gardner and was communicated to us by R. Houlgate and K. Codling. This remark applies to the Xe and Ne data used here and reported originally in Refs. 15 and 13, although the corrections in Ne were very small.

[28]T. E. H. Walker and J. T. Waber, J. Phys. B 7, 674 (1974).